

Catalytic Wet-Air Oxidation of *p*-Cresol on Ag/Al₂O₃–ZrO₂ Catalysts

Francisco Núñez,[†] Gloria Del Angel,^{*,†} Francisco Tzompantzi,[†] and Juan Navarrete[‡]

[†]Departamento de Química, Universidad Autónoma Metropolitana-Iztapalapa, Avenida San Rafael Atlixco No. 186, C. P. 09340, México D.F. México

[‡]Instituto Mexicano del Petróleo, Eje Central Lázaro Cárdenas 152, 07730 México, D.F. México

ABSTRACT: Catalytic wet-air oxidation of *p*-cresol was carried out on Ag/Al₂O₃–ZrO₂ catalysts at 1, 5, 10, and 20 wt % of ZrO₂ in a reactor-type batch and 160 °C and 15 bar of oxygen. Al₂O₃–ZrO₂ supports were prepared by the simultaneous hydrolysis of the boehmite and zirconium alkoxide. Ag/Al₂O₃–ZrO₂ catalysts prepared by deposition–precipitation showed higher surface area (202–216 m²/g) and lower Lewis acids sites than the Ag/Al₂O₃ (161 m²/g) and Ag/ZrO₂ (25 m²/g) reference catalysts. FTIR–CO adsorption showed a shift to lower frequencies on Ag/Al₂O₃–ZrO₂ catalyst indicating electron-rich metallic particles. The *p*-cresol conversion, TOC abatement, and CO₂ selectivity were improved when Ag was supported on Al₂O₃–ZrO₂ mixed oxides. A modification of the surface properties of Ag on the Ag/Al₂O₃–ZrO₂ catalysts due to a metal–support interaction leading to a faster oxidation of the adsorbed reactant species is proposed.

INTRODUCTION

Phenols are environmental pollutants present in discharge wastewaters from fossil fuel refining processes, phenol manufacturing plants, and a variety of industries. These phenolic compounds are toxic and nonbiodegradable by conventional methods, and the U.S. Resource Conservation and Recovery Act (RCRA), classifies the effluents containing phenols as highly dangerous.^{1,2} Processes such as the catalytic wet advanced oxidation route (CWAO) are favorable for converting the organic pollutants matter into carbon dioxide and water.^{3–6} In this way, metallic oxides like CuO have been successfully used as catalyst for the degradation of phenols (phenol, cresols, chlorophenols, nitrophenols, etc.) via CWAO.^{7,8} A combination of various metallic oxides as CuO–ZnO supported on alumina,⁹ CeO₂, or CeO₂ promoted with CuO and MnO, and noble metals as Rh and Pt have also been reported as good alternative catalysts for phenols degradation.^{10–14}

Catalytic wet-air oxidation on carbon support¹⁵ as well as transition metals oxides as FeO, Co₂O₃, NiO, and CuO provide efficient methods¹⁶ for phenol degradation. Support effects on noble metals were observed for CWAO of phenol; thus the support stabilizes the metallic surface area of Ru, Rh, Pt, Pd, Ag, and Au noble metals when they are supported on Al₂O₃, SiO₂, or TiO₂. The support provides high dispersion, enhanced activity, and stability^{4,6,16–21} to the active metal.

Zirconia, as a support, has also been used for the CWAO process in which Kraft-bleaching wastewater is successfully treated using Ru-supported on ZrO₂. However, zirconia has the disadvantage of having a very poor area.²² This takes into account that zirconia can be a good support for the CWAO process. In the present work the preparation of alternative supports for noble metals involving zirconium oxide was studied in the CWAO of *p*-cresol. Specifically, the catalytic wet-air oxidation of *p*-cresol, using silver supported on Al₂O₃–ZrO₂ mixed oxides (1, 5, 10, and 20 wt % ZrO₂) is reported. The characterization of the mixed oxides was made by means of nitrogen adsorption, XRD, H₂-TPR, FTIR-pyridine adsorption, and FTIR–CO chemisorption.

EXPERIMENTAL SECTION

The Al₂O₃–ZrO₂ mixed oxides were prepared at different contents of ZrO₂ (0, 1, 5, 10, 20 wt %) by means of a method that was named “boehmite peptization”. The method consists of the addition of a metallic alkoxide to the boehmite contained in an acid solution. The peptization of the boehmite and the alkoxide hydrolysis occurs simultaneously. With this method a strong interaction of the alkoxide with the Al–OH groups of the peptized boehmite is obtained, causing a high dispersion of ZrO₂ on the surface of alumina.

Supports and Catalysts Preparation. The γ-Al₂O₃ support was obtained by calcination of boehmite (CONDEA, high purity 99.999%, 74% AlOOH, 26% H₂O) under air flow (3.6 L/min) at 650 °C for 12 h.

Al₂O₃–ZrO₂ supports were prepared by boehmite peptization as follows: Catapal boehmita was put in contact with a solution containing 100 mL of butyl alcohol and the water stoichiometrically required to hydrolyze the zirconium alkoxide (Stream Chemicals 98%). For boehmite peptization the pH of the suspension was adjusted with nitric acid to a value of 3; afterward the temperature was increased to 80 °C under agitation for 12 h. Then the suspension was cooled down to room temperature, and the solution containing the Zr(OC₄H₉)₄ was added drop by drop in adequate amounts to obtain 0, 1, 5, 10, and 20 wt % of ZrO₂ in the Al₂O₃–ZrO₂ mixed oxides. The formation of the mixed oxide was then obtained by increasing the temperature to 100 °C under vigorous agitation and reflux, during 12 h. Afterward, the solids were dried in vacuum until dryness. Finally the solids were maintained in an oven at 120 °C for 12 h and then calcined under air flow at 650 °C for 6 h (60 mL min^{−1}).

Special Issue: IMCCRE 2010

Received: March 20, 2010

Accepted: July 12, 2010

Revised: July 5, 2010

Published: July 22, 2010

Ag/Al₂O₃–ZrO₂ catalysts preparation was carried out by deposition–precipitation (2 wt % Ag nominal). The support was put in contact with a solution of AgNO₃ at a concentration of 2.35×10^{-2} M. Then the pH was fitted to 6.8 by the addition of a KOH solution (0.1 and 0.01 M) to precipitate the Ag⁺ ions on the support.²³ The suspension was heated up then to 80 °C and kept under vigorous agitation, for 8 h. Afterward the solids were separated by filtration, and then washed with 100 mL of distilled water. This operation was repeated four times. Then, the solids were dried to 120 °C overnight and calcined at 300 °C under air flow for 4 h. Finally, the catalysts were reduced under hydrogen flow at 300 °C for 4 h; afterward, the samples were stored in a desiccator with vacuum. For identification, samples were labeled as Al₂O₃–ZrO₂X (where X represents the weight % of the ZrO₂).

Characterization. The specific surface area of the supports was determined from the nitrogen adsorption isotherms (Brunauer–Emmett–Teller (BET) method) using a Quantachrome Autosorb-3B equipment. Pore mean size diameter distribution was determined from the desorption isotherms and calculated by means of the Barret–Joyner–Halenda (BJH) method.

The X-rays diffraction pattern of the γ -Al₂O₃, γ -Al₂O₃–ZrO₂, and ZrO₂ supports were obtained with a SIEMENS D-500 diffractometer with anode of Cu and monocromador of secondary beam. The identification of the compounds was made using the JCPDS reference cards 10-0425, 14-0534 D, and 7-0343 corresponding to γ -Al₂O₃ and ZrO₂ crystalline phases, respectively.

The type and amount of acid sites (Brönsted and/or Lewis) on the supports were determined by pyridine adsorption infrared spectroscopy (FTIR) study using a Nicolet 170 SX instrument with Fourier transformation. The solid material was pressed into thin self-supported wafers. Then, they were placed in a glass Pyrex cell with CF₂ windows coupled to a vacuum line, in order to be evacuated (1×10^{-6}) in situ at 400 °C for 30 min. The pyridine adsorption was carried out in the cell at 25 °C. Afterward the adsorbed pyridine was desorbed with vacuum from room temperature to 400 °C on intervals of 100 °C. The quantities of the remaining adsorbed pyridine were obtained from the integrated absorbance bands, following the procedure and using the extinction coefficient reported elsewhere.²⁴

H₂-TPR experiments were made in a CHEMBET-3000 (QUANTACHROME Co) equipment using 0.2 g of catalyst by means of the following protocol: samples were heated at 300 °C under nitrogen flow (10 mL min⁻¹) during 30 min. Then, the samples were cooled down to room temperature. A mixed gas flow (5% H₂/95% N₂) was passed then through the cell. The TPR profiles were registered using a heating program of 10 °C min⁻¹ from room temperature to 700 °C using a flow rate of the gas mixture of 10 mL/min.

The CO chemisorbed FTIR spectra were obtained at room temperature using a Nicolet-FX710 apparatus. The samples pressed in thin wafers were placed in a Pyrex glass cell equipped with CaF₂ windows. The samples were pretreated *in situ* under hydrogen flow at 300 °C for 30 min, then the samples were cooled down to room temperature and a N₂ flow was passed through the samples during 30 min, after CO was introduced to the system for 30 min and then the FTIR spectra were registered.

The oxidation reactions were performed in a 500 mL batch reactor of stainless steel high-pressure (Parr Instrument Co Ltd., IL) coated with a glass linear to prevent corrosion problems. The reactor includes a stirrer, gas supply system, and temperature controller. In a typical experiment, the reactor was loaded with

Table 1. Specific Surface and Mean Pore Size Diameter for Al₂O₃, ZrO₂, and Al₂O₃–ZrO₂ Supports

support	mean pore diameter (Å)	specific surface area (m ² g ⁻¹)
Al ₂ O ₃	122	161
Al ₂ O ₃ –ZrO ₂ 1%	94	216
Al ₂ O ₃ –ZrO ₂ 5%	90	215
Al ₂ O ₃ –rO ₂ 10%	76	212
Al ₂ O ₃ –rO ₂ 20%	76	202
ZrO ₂	25	25

300 mL of a solution containing 1000 ppm of *p*-cresol and 1 g/L of catalyst. The system was then heated to the reaction temperature and pressurized with air under continuous stirring of 750 rpm. Time zero was defined when the preset conditions were attained (temperature, 160 °C; oxygen pressure, 15 bar). Periodically, at time intervals of 15 min, samples (10 mL) were withdrawn from the reactor using the sampler valve and analyzed by gas chromatography on a capillary column DB-WAX, 30 m, 0.53(ID), 1.0 μ m of film. During the chromatographic analysis 4-methylcatechol, 4-hydroxybenzaldehyde, and 4-hydroxybenzyl alcohol were identified.

To complete the carbon balance, total organic carbon (TOC) was determined using a 5000 TOC Shimadzu analyzer. The selectivity toward CO₂ was calculated using the following relation:¹⁰ $SCO_2 = (X_{TOC}/X_{p-cresol}) \times 100$, where $X_{TOC} = [(TOC_o - TOC)/TOC_o] \times 100$; TOC_o = TOC value at $t = 0$ and TOC = value at different t ; $X_{p-cresol}$ = conversion of *p*-cresol (%). The initial rate (in mmol h⁻¹ g_{cat}⁻¹) was calculated using the TOC conversion values $r_i = (\Delta TOC(\%)/\Delta t) ([pollutant]_i \times m_{cat})$, where: $(\Delta TOC(\%)/\Delta t)$ = initial slop obtained from the TOC conversion as function of time curves; $[pollutant]_i$ = initial concentration of the pollutant and m_{cat} = mass of catalyst.

RESULTS AND DISCUSSION

The specific surface area (BET) and mean pore diameter of the supports are reported in Table 1 where it can be seen that addition of ZrO₂ to the alumina increases the specific area of the reference supports. For Al₂O₃ and ZrO₂ the BET areas were 161 m² g⁻¹ and 25 m² g⁻¹, respectively, while for the mixed oxides the BET areas increase to 216, 215, 212, and 202 m² g⁻¹ for 1, 5, 10, and 20 wt % of ZrO₂ content in the mixed oxide, respectively. The increase in the specific area showed by the mixed oxides can be explained by the preparation method used. The zirconium butoxide was added during preparation to peptized boehmite producing a strong modification in the hydrolysis–condensation reactions occurring in both peptized boehmite and zirconium alkoxide. Thus the textural properties of the mixed oxides were notably improved. The Al₂O₃–ZrO₂ mixed oxides show mean pore diameters between 94–76 Å, which are between the 122 and 25 Å showed for Al₂O₃ and ZrO₂ reference supports, respectively. On silver-containing supports any substantial modification on the specific surface areas or mean pore diameter was noted.

XRD diffractograms for Ag/Al₂O₃, Ag/ZrO₂, and Ag/Al₂O₃–ZrO₂ catalysts are shown in Figure 1. For alumina the X-ray diffraction pattern shows the characteristic peaks for γ -Al₂O₃ at 2θ : 30, 46, and 68. On the other hand, for ZrO₂ the X-ray diffraction pattern shows three peaks in 2θ : 30, 50.5, and 60.3 which correspond to the tetragonal crystalline structure of zirconium oxide accompanied by peaks at 2θ : 28.3 and 31.6,

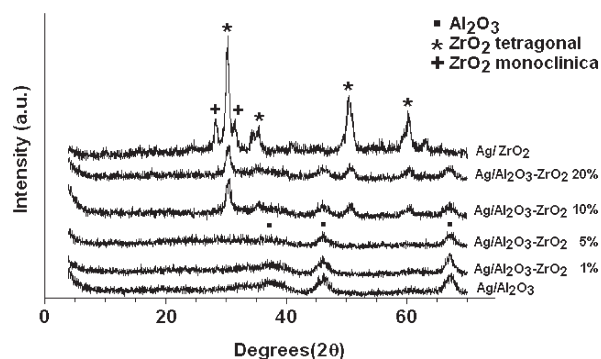


Figure 1. XRD patterns of the Ag-supported catalysts.

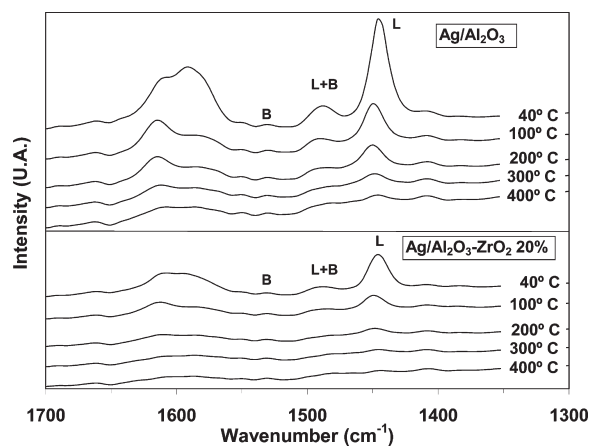


Figure 2. FTIR spectra of pyridine adsorption on Ag/Al₂O₃ and Ag/Al₂O₃-ZrO₂20% catalysts.

which are assigned to the zirconia monoclinic crystalline structure.²⁵ Then a mixture of the monoclinic and tetragonal crystalline structures were obtained in the ZrO₂ reference sample. For the catalysts containing 1 and 5% of ZrO₂ only the peaks identifying γ -alumina can be observed, suggesting that ZrO₂ is well dispersed on the Al₂O₃ support and hence cannot be detected by XRD due to the small size of the conglomerates. For the mixed oxides at high ZrO₂ content (10 and 20 wt %), the diffractograms showed the peaks identifying γ -alumina and tetragonal ZrO₂. No peaks corresponding to zirconium oxide with monoclinic crystalline structure were detected. Thus the alumina inhibited the formation of the monoclinic form and stabilized the tetragonal structure. In the XRD patterns the peaks corresponding to silver should be placed at 2θ : 38, 44, 65, and 78; however, they cannot be seen. This can be due either to the wavelength of the peaks corresponding to metallic Ag, which appears very close to the alumina signals, where alumina is probably masking the silver peaks or to such a low concentration of Ag that it cannot be detected by this technique.^{26,27}

The pyridine adsorbed FTIR spectra as a function of the temperature for two selected samples, Ag/Al₂O₃ and Ag/Al₂O₃-ZrO₂10% are shown in Figure 2. Pyridine adsorption has been reported as a good method to determine the properties and nature of the sites (Lewis or Brønsted) on metal oxides. The FTIR pyridine absorption spectra on Ag/Al₂O₃ shows an absorption band at 1445 cm⁻¹ which has been assigned to the adsorption of pyridine coordinated on Lewis acid sites and two

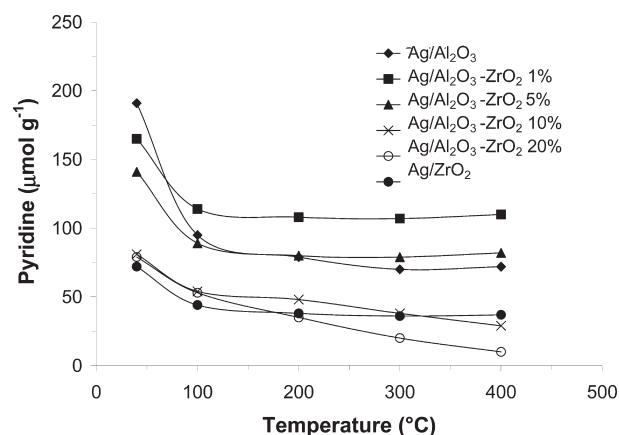


Figure 3. Pyridine adsorbed as a function of the desorption temperature for the Ag supported catalysts.

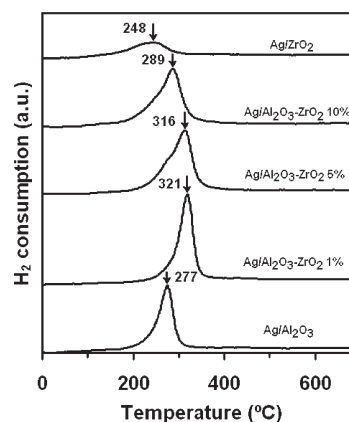


Figure 4. H₂ uptake profiles during the TPR experiments of the Ag supported catalysts.

absorption bands at 1490 and 1600 cm⁻¹ associated to the presence of Lewis and Brønsted acid sites and the weak Lewis acid sites, respectively. It must be noted that the band at 1545 cm⁻¹ assigned Brønsted acid sites is not present on these catalysts. In Figure 2, it can be observed that the bands intensity decreases as desorption temperature increases. The amount of adsorbed pyridine ($\mu\text{mol g}^{-1}$) for the different Ag supported catalysts as a function of the desorption temperature are shown in Figure 3. The addition of ZrO₂ to alumina on the Ag/Al₂O₃-ZrO₂ catalysts produces a decrease in the total acidity. It can be assumed that a modification on the acid strength and distribution occurs in the Al₂O₃-ZrO₂ mixed oxides. This modification could affect the adsorption properties of the Ag deposited on the surface of these mixed oxide solids.

The H₂-TPR thermograms for various solids are shown in Figure 4. It can be observed that Ag on Al₂O₃-ZrO₂ mixed oxides presents a higher temperature of reduction of around 289–321 °C with respect to Ag supported on Al₂O₃ (277 °C) and ZrO₂ (248 °C). The shift to higher reduction temperatures can be related to the stabilization of Ag on the larger surface area shown by the mixed oxide supports.

Infrared spectra of chemisorbed CO on Ag for two selected catalysts are shown in Figure 5 and the corresponding infrared frequencies (ν) for all the catalysts are reported in Table 3. The

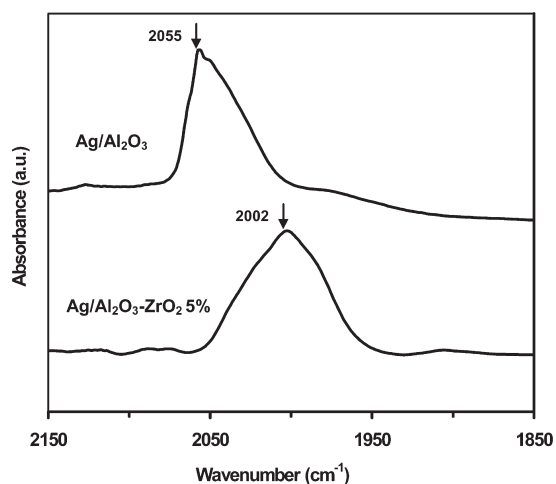


Figure 5. FTIR spectra of CO adsorbed on Ag/Al₂O₃ and Ag/Al₂O₃-ZrO₂ 5% catalysts.

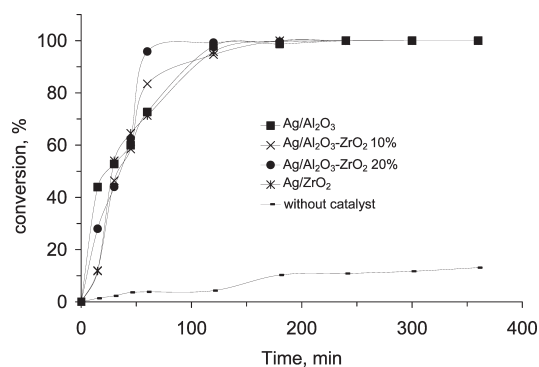


Figure 6. CWAQ of *p*-cresol on Ag/catalysts ($T = 160\text{ }^{\circ}\text{C}$; $P_{\text{O}_2} = 15\text{ bar}$).

Table 2. Activity and Selectivity for the Catalytic Wet-Air Oxidation of *p*-Cresol after 1 h of Reaction^a

catalyst	r_i^b (mmol h ⁻¹ g _{cat} ⁻¹)	abatement TOC (%)	<i>p</i> -cresol conversion (%)	selectivity to CO ₂ (1 h) (%)
Ag/Al ₂ O ₃	0.7	13	73	18
Ag/Al ₂ O ₃ -ZrO ₂ 1%	2.1	21	56	37
Ag/Al ₂ O ₃ -ZrO ₂ 5%	3.0	34	65	61
Ag/Al ₂ O ₃ -ZrO ₂ 10%	4.9	40	77	51
Ag/Al ₂ O ₃ -ZrO ₂ 20%	14.0	50	96	52
Ag/ZrO ₂	1.1	9	71	12

^a $P(\text{O}_2) = 15\text{ bar}$, catalyst = 1 g L^{-1} , $[\text{C}_7\text{H}_8\text{O}]_i = 9.3\text{ mmol L}^{-1}$. ^b Initial rate of TOC conversion.

Ag supported on alumina and zirconia present absorption bands at 2055 and 2031 cm⁻¹ respectively, whereas, for Ag supported on Al₂O₃-ZrO₂ mixed oxides, the bands are shifted to lower frequencies, 2012–2002 cm⁻¹. This behavior can be attributed to differences on the Ag surface properties due to interactions with supports having different textural properties. It can be assumed that on Ag/Al₂O₃ and Ag/ZrO₂ the Ag particles have different electron density to that of silver deposited on Al₂O₃-ZrO₂ mixed oxides.

Table 3. Infrared Frequencies (ν , cm⁻¹) for Chemisorbed CO on Ag-Supported Catalysts

Ag/Al ₂ O ₃	2055
Ag/Al ₂ O ₃ -ZrO ₂ 5%	2002
Ag/Al ₂ O ₃ -ZrO ₂ 10%	2012
Ag/Al ₂ O ₃ -ZrO ₂ 20%	2010
Ag/ZrO ₂	2031

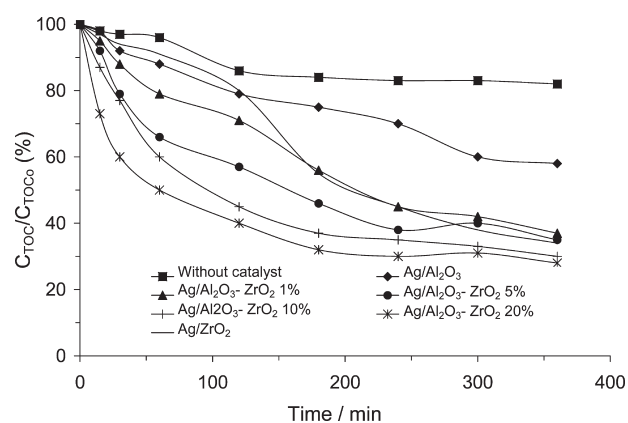


Figure 7. Normalized TOC concentration reduction (%) as a function of time for Ag-supported catalysts in *p*-cresol CWAQ.

In Figure 6 the conversion of *p*-cresol as a function of time for the various catalysts is shown, where an undefined behavior can be observed. However, since the *p*-cresol degradation in absence of catalyst is practically null, the catalytic effect of the silver catalysts can clearly be seen. Total oxidation of *p*-cresol for all the catalysts is reached after 2 or 3 h of reaction (Figure 6).

To disclose the support effect in the *p*-cresol in Table 2 conversions after 1 h of reaction are reported. For Ag/Al₂O₃ and Ag/ZrO₂, catalysts conversions of 73 and 71%, respectively, were obtained, while a maximum conversion up to 96% is obtained with the Ag/Al₂O₃-ZrO₂ 20% catalyst. The *p*-cresol degradation as a function of time is a good indicator of the activity of the catalysts. However, the determination of the remaining total organic compounds in the solution containing the pollutant compound indicates the selectivity of the catalysts for the total conversion of organic compound to CO₂ and H₂O. Normalized TOC concentration reduction as a function of time for the various catalysts is shown in Figure 7. The initial rates (at $t = 0$) calculated from Figure 7 are reported in Table 2.

Higher initial rates were obtained with the mixed oxides when compared with Al₂O₃ or ZrO₂ reference catalysts. In Table 2 a notable high activity for catalysts containing 20 wt % of ZrO₂ can be seen. TOC abatement and selectivity to CO₂ after 1 h of reaction are also reported in Table 2. The better TOC abatement of 50% and the highest mineralization to CO₂, 61%, was obtained with the Ag/Al₂O₃-ZrO₂ catalysts. Figure 8 shows the percentage of mineralization to CO₂, where a maximum of selectivity to CO₂ in Ag/Al₂O₃-ZrO₂ catalysts can be observed.

The high activity and selectivity presented by Ag/Al₂O₃-ZrO₂ catalysts can be due to different metal-support interaction-inducing modifications in the electronic density of silver particles. According to the CO absorption FTIR spectra Ag surface particles on Al₂O₃-ZrO₂ are electron-rich, whereas on alumina and zirconia simple oxides the Ag surface particles are electron deficient. The adsorption of the reactant molecule on

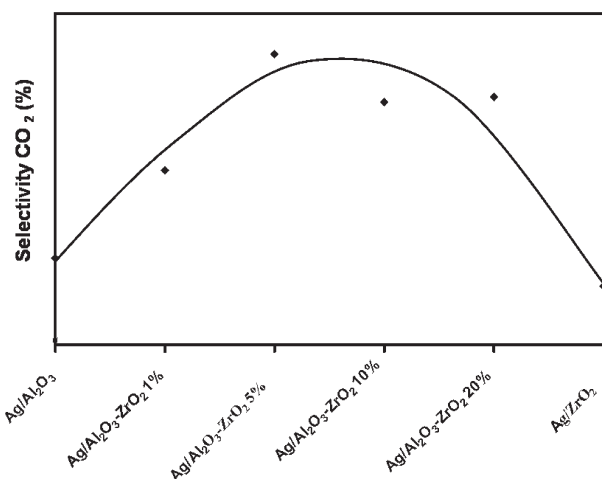


Figure 8. Selectivity to CO₂ for Ag/Al₂O₃, Ag/ZrO₂, and Ag/Al₂O₃–ZrO₂ catalysts in *p*-cresol CWAQ.

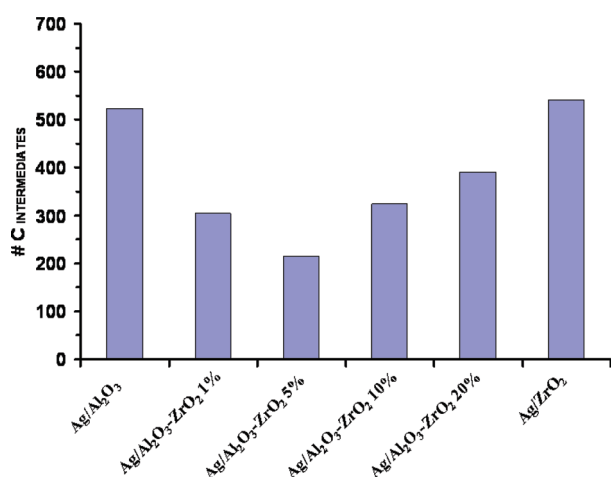


Figure 9. Number of intermediate carbons after 1 h of reaction for Ag/Al₂O₃, Ag/ZrO₂, and Ag/Al₂O₃–ZrO₂ catalysts in *p*-cresol CWAQ.

the Ag/Al₂O₃–ZrO₂ surface was favored, and therefore a faster oxidation of the adsorbed species occurred and an increase in the activity and degradation of the pollutant was obtained. Since the total degradation of *p*-cresol was not attained even after 3 h of reaction, the number of the intermediates (4-methylcatechol, 4-hydroxybenzaldehyde, 4-hydroxybenzylalcohol) remaining in the polluted solution is reported in Figure 9. A low concentration of byproduct with Ag/Al₂O₃–ZrO₂ catalysts was found. These results are in agreement with previous data reported in the literature for different catalysts,²⁸ in which 4-hydroxyphenyl alcohol was obtained by oxidation of the methyl group of *p*-cresol, followed by the formation of 4-hydroxybenzaldehyde. It is also proposed that the intermediate 4-methylcatechol is obtained by oxidation at the ortho position of the aromatic ring with respect to the hydroxyl group of the *p*-cresol.²⁹

CONCLUSIONS

Al₂O₃–ZrO₂ mixed oxides showing high specific surface areas were obtained by simultaneous peptization of boehmite and zirconium alkoxide hydrolysis. Ag/Al₂O₃–ZrO₂ catalysts with lower acidity than Ag/Al₂O₃ and Ag/ZrO₂ catalysts were

obtained. A modification of the Ag adsorption properties were detected on the Ag/Al₂O₃–ZrO₂ catalysts. Improved activity for the *p*-cresol catalytic wet-air oxidation was observed with the Ag/Al₂O₃–ZrO₂ catalysts. Higher selectivity to CO₂ was reached in the catalyst at high zirconia content. The higher activity showed by the Ag/Al₂O₃–ZrO₂ catalyst is explained by the metal support interaction occurring between the mixed oxides and deposited silver.

AUTHOR INFORMATION

Corresponding Author

*Tel.: (55)5804-4668. Fax: (55)5804-4666. E-mail: gdam@xanum.uam.mx.

ACKNOWLEDGMENT

F. Nuñez thanks CONACYT for a scholarship.

REFERENCES

- (1) William, D. C.; Rothschild, W. Wet-air oxidation of spent caustics. *Nat. Environ. J.* **1994**, *4* (6), 16.
- (2) Kumaran, P.; Paruchuri, Y. L. Kinetics of phenol biotransformation. *Water Res.* **1997**, *31*, 11.
- (3) Luck, F. Wet-air oxidation: Past, present and future. *Catal. Today* **1999**, *53*, 81.
- (4) Gómez, H. T.; Orfao, J. J. M.; Figueiredo, J. L. CWAQ of butyric acid solution: Catalyst deactivation analysis. *Ind. Eng. Res.* **2004**, *43*, 1216.
- (5) Gallezot, P.; Chaumet, S.; Perrat, A.; Isnard, P. Catalytic wet-air oxidation of acetic acid on carbon-supported ruthenium catalysts. *J. Catal.* **1997**, *168*, 104.
- (6) Duprez, D.; Delanoë, F.; Barbier, J.; Isnard, P. Catalytic oxidation of organic compounds in aqueous media. *Catal. Today* **1996**, *29*, 317.
- (7) Arena, F.; Giovenco, R.; Torre, T.; Venuto, A.; Parmaliana, A. Activity and resistance to leaching of Cu-based catalysts in the wet oxidation of phenol. *Appl. Catal., B* **2003**, *45*, 51.
- (8) Santos, A.; Yustos, P.; Rodríguez, S.; García, F. Wet oxidation of phenol, cresols and nitro phenols catalysed by activated carbon in acid and basic media. *Appl. Catal., B* **2006**, *65*, 269.
- (9) Pintar, A.; Levec, J. Catalytic oxidation of organics in aqueous solution: Kinetics of phenol oxidation. *J. Catal.* **1992**, *135*, 345.
- (10) Lin, S. S.; Chang, D. J.; Wang, C. H.; Chen, C. C. Catalytic wet-air oxidation of phenol by CeO₂ catalyst—Effect of reaction conditions. *Water Res.* **2003**, *37*, 793.
- (11) Shido, T.; Iwasawa, Y. Reactant-promoted reaction mechanism for water–gas shift reaction on Rh-doped CeO₂. *J. Catal.* **1993**, *141*, 71.
- (12) Hilaire, S.; Wang, X.; Luo, T.; Gorte, R. J.; Wagner, J. A comparative study of water–gas-shift reaction over ceria-supported metallic catalysts. *Appl. Catal., A* **2001**, *215*, 271.
- (13) Jacobs, G.; Graham, U. M.; Chenu, E.; Patterson, P. M.; Dozeir, A.; Davis, B. H. Low-temperature water gas shift impact of Pt promoter loading on the partial reduction of ceria and consequences for catalyst design. *J. Catal.* **2005**, *229*, 499.
- (14) Chen, I. P.; Lin, S. S.; Wang, C. H.; Chang, L.; Chang, J. S. CWAQ of phenol using CeO₂/Al₂O₃ with promoter—Effectiveness of promoter addition and catalyst regeneration. *Chemosphere* **2007**, *66*, 172.
- (15) Suarez, M. E.; Stuber, F.; Fortuny, A.; Fabregat, A.; Carrera, J.; Font, J. Catalytic wet-air oxidation of substituted phenols using activated carbon as catalyst. *Appl. Catal., B* **2005**, *58*, 105.
- (16) Levec, J.; Pintar, A. Catalytic oxidation of aqueous solutions of organics. An effective method for removal of toxic pollutants for waste waters. *Catal. Today* **1995**, *24*, 51.
- (17) Qin, J.; Aikc, K. J. Catalytic wet-air oxidation of ammonia over alumina-supported metals. *Appl. Catal., B* **1998**, *16*, 261.

- (18) Barbier, J., Jr.; Oliviero, L.; Renard, B.; Duprez, D. Catalytic wet-air oxidation of ammonia over M/CeO₂ catalysts in the treatment of nitrogen-containing pollutants. *Catal. Today* **2002**, 75, 29.
- (19) Ukropec, R.; Kuster, B.; Shouten, J.; Van Santen, R. Low temperature oxidation of ammonia to nitrogen in liquid phase. *Appl. Catal., B* **1999**, 23, 45.
- (20) Taguchi, J.; Okuhara, T. Selective oxidative decomposition of ammonia in neutral water to nitrogen over titania-supported platinum or palladium catalyst. *Appl. Catal., A* **2000**, 194/195, 89.
- (21) Aguilar, C.; García, R.; Soto, G.; Arriganaga, R. Catalytic wet-air oxidation of aqueous ammonia with activated carbon. *Appl. Catal., B* **2003**, 46, 229.
- (22) Pintar, A.; Besson, M.; Gallezot, P. Catalytic wet-air oxidation of Kraft bleaching plant effluents in the presence of titania and zirconia supported ruthenium. *Appl. Catal., B* **2001**, 30, 123.
- (23) Sano, T.; Negishi, N.; Mas, D.; Takeuchi, K. Photocatalytic decomposition of N₂O on highly dispersed Ag⁺ ions on TiO₂ prepared on photodeposition. *J. Catal.* **2000**, 194, 71.
- (24) Emeis, C. A. Determination of integrated molar extinction coefficients for infrared absorption bands of pyridine adsorbed on solid acid catalysts. *J. Catal.* **1993**, 141, 347.
- (25) Grau, J. M.; Roman, C.; Parera, J. M. Alternatives for a better performance of Pt in SO₄²⁻/ZrO₂ mixed or supported onto Al₂O₃ and SiO₂. *Appl. Catal., A* **1998**, 172, 311.
- (26) Ngamsom, B.; Bogdanchikova, N.; Borja, A. M. Characterization of Pt–Ag/Al₂O₃ catalysts for selective acetylene hydrogenation: effect of pretreatment with NO and N₂O. *Catal. Commun.* **2004**, 5, 243.
- (27) Shinizu, K.; Hashimoto, M.; Shibata, J.; Hattori, T.; Satsuma, A. Effect of modified alumina supports on propane–hydrogen–SCR over Ag/alumina. *Catal. Today* **2006**, 126, 266.
- (28) Zhenghong, G.; Jing, S. Y.; Siping, W.; Ping, Y. The effect of different resin supports on activity and stability of Co catalysts for the oxidation of *p*-cresol to *p*-hydroxybenzaldehyde. *Appl. Catal., A* **2001**, 209, 27.
- (29) Santos, A.; Yustos, P.; Rodriguez, S.; Garca-Ochoa, F. Wet-air oxidation of phenol, cresols, and nitrophenols catalyzed by activated carbon in acid media and basic media. *Appl. Catal., B* **2006**, 65, 269.